



OPEN

Determination of behavior of catalpol hexapropionate in simulated gastric conditions by UPLC–ESI–HRMS

Xiaodong Cheng¹, Qiuxia Zhang^{1,2}, Zhenxing Li¹, Chunhong Dong³✉, Shiqing Jiang³, Yu-an Sun¹ & Guoqing Wang¹✉

Catalpol hexapropionate (CP-6) was designed and synthesized as anti-aging drug. In order to investigate the behavior of CP-6 in simulated gastric juice, ultra-high performance liquid chromatography–electrospray ionization–high resolution mass spectrometry was used to determinate the components produced in simulated gastric conditions. Six metabolites were identified with the possible metabolic processes proposed. Hydrolysis may be the main metabolic pathways. The relative contents of CP-6 and its metabolites were determined using their extractive ion chromatograms. The results show that the relative content of CP-6 is rapidly decreased about 15% during the first 0.5 h and generally stable after 0.5 h. The mainly produced metabolites are catalpol penta-propionate (CP-5), catalpol and a spot of catalpol tetra-propionate (CP-4), catalpol tri-propionate (CP-3), catalpol dipropionate (CP-2) and catalpol propionate (CP-1). The metabolic process of CP-6 may be an hydrolysis under acid conditions. The research results can provide useful information for development and utilization of CP-6 as a pharmaceutical preparation.

Catalpol is a small molecular of iridoid glycoside which can be derived from fresh or dried root of the *rehmannia glutinosa* Libosch¹. In recent years, catalpol has been paid more and more attention because of its extensive pharmacological activities. A large number of studies have shown that catalpol has a good pharmacological activity in improving cardiovascular, cerebrovascular, central-nervous system diseases and boosting immunity, regulating blood glucose and lipid metabolism, anti-tumor, anti-osteoporosis, anti-inflammation^{2–13}. However, the application of catalpol was severely limited in clinic because of its short half-life in vivo and high water solubility, it is difficult to penetrate the blood–brain barrier¹⁴. In order to improve its druggability, the structure of catalpol can be modified by esterification, and we previously introduced propionic anhydride to obtain catalpol propionylated derivatives, and the molecular docking study (MD) and MTT analysis showed that the catalpol hexapropionylation derivative (CP-6) maybe with the highest anti-aging effect^{15,16}.

It is known that the metabolism of oral drugs in the gastrointestinal tract will directly affect the amount of maternal drugs in the digestive tract, in which drugs may undergo chemical degradation or enzyme degradation, thus reducing the amount of maternal drugs and reducing their bioavailability^{17,18}. The methods of drug metabolism research include two methods: in vivo research and in vitro research. Because of the simplicity and rapidity of in vitro metabolism research, it was more and more used to detect the complex physical and chemical changes of drugs in the digestive tract, especially the conjecture of their metabolic pathways and the identification of metabolites. The conventional methods for in vitro metabolic studies include high performance liquid chromatography (HPLC–UV), micellar electric capillary chromatography–mass spectrometry (MECC–MS), gas chromatography–mass spectrometry (GC–MS), GC–MS/MS and liquid chromatography–mass spectrometry (LC–MS) or LC–MS/MS^{19–24}. In these methods, the metabolites should be previously separated by GC or LC, and then be identified by UV, MS or MS/MS methods. These pre-separated or MS/MS identified procedures are usually time consuming.

¹School of Materials and Chemical Engineering, Zhengzhou University of Light Industry, Zhengzhou, China. ²School of Chemical and Environmental Engineering, Pingdingshan University, Pingdingshan, China. ³Henan University of Chinese Medicine, Zhengzhou, China. ✉email: chunhong_dong@hactcm.edu.cn; gqwang@zzuli.edu.cn

In this work, using UPLC as means of separation and sampling device, ESI as ionizing device characteristic with no gas ionized debris, and Orbitrap-Exactive high resolution mass spectrometer (HRMS) for accurate determination of molecular mass of organic compounds²⁵, the metabolic process of CP-6 in simulated gastric conditions was determined, and the determined metabolites may provide useful information for the development and utilization of CP-6 as pharmaceutical preparation.

Experimental

Materials and reagents. Catalpol hexapropylate was laboratory homemade and purified (CP 98%). Chromatographic pure reagent MeOH, CH₃CN and ethyl acetate were purchased from Tianjin Siyou Fine Chemicals Co. Ltd., China. Ultrapure water was prepared by Mill-QAdvantage A10 ultrapure water meter (Millipore, USA). Pepsin (Saiguo Biotechnology Co. Ltd., China, 1:10,000). Trypsin (Jiangsu Kaiji Biotechnology Co. Ltd., China, 1:250). HCl (Nanjing Chemical Reagent Co. Ltd., China, AR 36.0%-38.0%). NaOH (Xilong Chemical Co. Ltd., China, AR 99%). KH₂PO₄ (Nanjing Chemical Reagent 1st Plant, China, AR 99%).

Standard stock solution of CP-6 (2 mg/mL) was prepared using 200 mg CP-6 and MeOH to dissolve with the final volume completed to 100 mL.

Simulated gastric juice was prepared using 0.70 mL HCl, 0.20 g NaCl and 0.32 g pepsin which dissolved in distilled water, and the final solution is completed constant volume to 100 mL with distilled water. The resulting solution with a pH value of ~ 1.2 was maintained at 37 °C and stirred continuously^{21,26}.

Apparatus. Waters ACQUITY Ultra High Performance Liquid Chromatograph coupled with Thermo Fisher-Exactive Orbitrap high resolution mass spectrometer (HRMS) was used for simulated gastric juice and simulated intestinal fluid analysis. DF-101 SA-H collecting heating at constant temperature magnetic stirrer (Nanjing Kohl Instruments and Equipment Co. Ltd., China), 80-2 Electric Centrifuge (Changzhou Guoyu Instruments Manufacturing Co. Ltd., China).

UPLC conditions: Waters ACQUITY UPLC with Wakopak ultra C18-3 (3.0 mm × 250 mm) column and PDA detector.

HRMS conditions: ESI ionization source; automatic sampler mobile phase ratio, acetonitrile:0.1% aqueous formate solution (V:V) = 60:40; flow rate, 200 µL/min; capillary temperature, 250 °C; capillary tube voltage, 60 V; tube voltage, 120 V; injection volume, 0.1 µL; auxiliary gas, 10 L/min; sheath gas, 40L/min; skimmer voltage, 22 V; sketch time, 2 min; scan range/(m/z), 100–1,000, electronic transmission tube temperature, 275 °C; scanning mode, positive and negative ions scanning mode respectively.

Determination of the metabolites. 2 mL stock solution of CP-6 prepared in section *Materials and Regent* was added to 5 mL simulated gastric juice which were placed at 37 °C thermostatic bath. Respectively sampling 200 µL at 0, 0.05, 0.5, 1.0, 1.5, 2.0, 2.5, 3.0, 3.5 and 4.0 h, adding 0.2 mol/L NaOH solution to adjust pH ~ 7, adding 1 mL MeOH and mixing to deactivate the enzyme^{21,26}. Centrifugated 1,000 r/min for 15 min, filtered with 0.22 µm PTFE microporous membrane, then 0.1 µL filtered solution was analyzed using the optimal UPLC-ESI-HRMS conditions.

Results and discussion

Selection of ion scanning mode. The ionization pattern has a significant effect on the detection and characterization of analytes in the samples. In this study, positive ionization (PI) and negative ionization (NI) modes were tried: Fig. 1 shows TIC of CP-6 under the simulated gastric juice for 3 h at negative scanning mode (Upper section) and positive scanning mode (Lower section). Figure 2 is the HRMS in PI mode at a retention time of 6.58 min. M/z 699.2803 and m/z 716.3064 are the [M + H]⁺ peak and [M + NH₄]⁺ peak of CP-6, respectively. It can be seen that there is no obvious peak of CP-6 at retention time ~ 6.5 min, and therefore the PI mode was selected in this study.

Possible metabolic processes and accurate molecular weight of metabolic debris. Based on the structure and synthesis procedure of CP-6, the possible metabolic process may be esterlysis of CP-6 that shown as Fig. 3.

In Fig. 3, the metabolites CP-5, CP-4, CP-3, CP-2, CP-1 and catalpol were produced by the hydrolysis of CP-6 and then the loss of 1 to 6 C₃H₄O⁻, i.e., loss of CH₃CH₂COO⁻ and add an H⁻, respectively. The chemical formula and theoretical mass of ionized debris of the possible metabolites and CP-6 was shown in Table 1.

Metabolites identification and semi-quantification. Since ESI is a typical “soft ionization” mode, generally does not occur decomposition during ionization, so we can identify the possible metabolites in mixtures by cross validation of their theoretical m/z of [M + H]⁺, [M + NH₄]⁺, and [M + Na]⁺.

Metabolites identification. Take the identification of CP-5 as an example. Figure 4 shows HRMS of mixed peak at certain time. It can be seen that the experimental measured m/z 643.2546, 660.2810 and 665.2362 appeared that can be respectively to that the theoretical m/z [M + H]⁺, [M + NH₄]⁺ and [M + Na]⁺ as 643.2602, 660.2862 and 665.2416 shown in Table 1, and the absolute deviations between the experimental and theoretical are less than 0.01. According to theoretical m/z of possible metabolites at PI mode, the experimental m/z of the metabolites were obtained and shown as Table 2. The identified metabolites are CP-5, CP-4, CP-3, CP-2, CP-1 and catalpol, which may be produced by the hydrolysis process of CP-6, or produced by esterificaion of the metabolites catalpol and propionic acid.

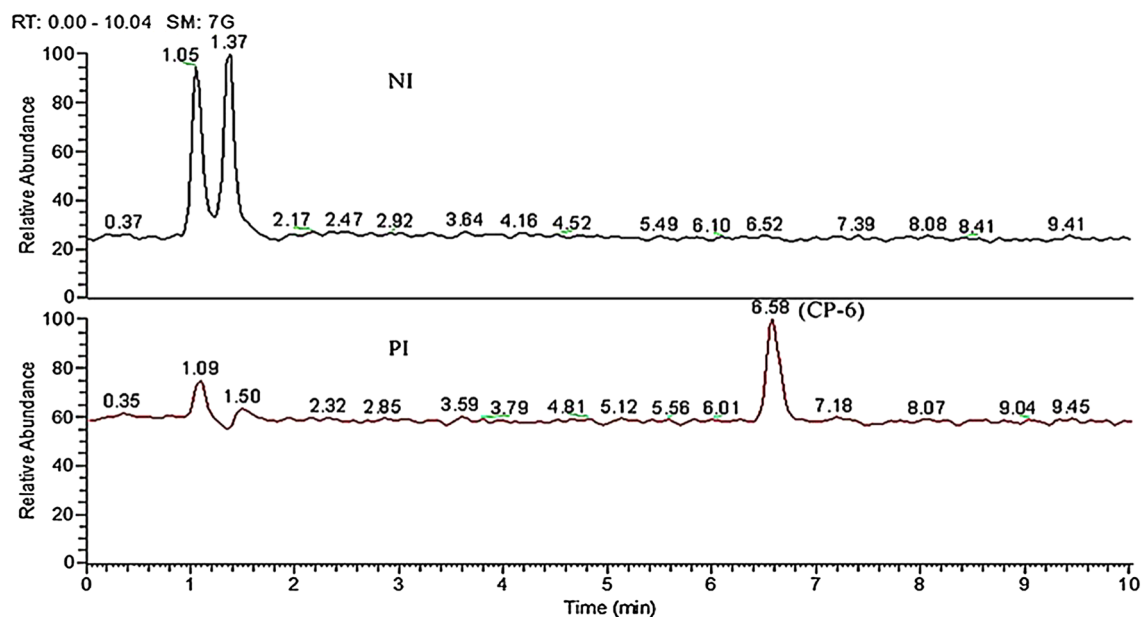


Figure 1. TIC of metabolites analyzed at NI mode and PI mode.

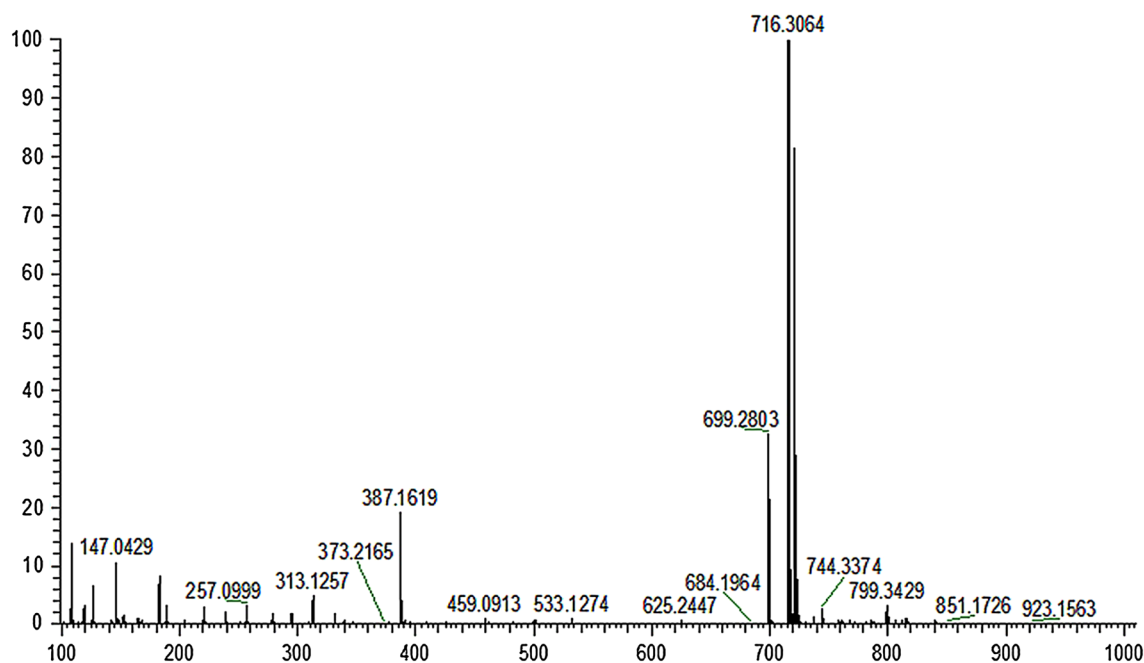


Figure 2. HRMS in PI mode at a retention time of 6.58 min.

Metabolites quantification. Because of the similar structures, the metabolites are difficult to be separated by UPLC. Although three metabolites were identified, the TIC peaks analysis of the metabolites are mainly at time (min) 1.09, 1.50 and 6.58. In order to quantify the metabolites, extracted ion chromatograms (EIC) of metabolites m/z $[M+H]^+$, $[M+NH_4]^+$ and $[M+Na]^+$ shown as Table 2 were used. The relative contents of the peak areas of the metabolites can represent their relative contents at certain time. Figure 5 shows EIC of the metabolites that CP-6 under the simulated gastric juice for 3 h. It should be noticed that the EIC of CP-5, CP-4, CP-3, CP-2 and CP-1 are with multiple peaks, and this is due to these components are multiple isomers¹⁵.

Table 3 shows the relative content changes of the metabolites within 4 h of CP-6 under the simulated gastric juice conditions using EIC mode based on the relative peak areas of the selected metabolites.

It can be seen from Table 3 that CP-6 is unstable in the simulated gastric juice conditions, and the main metabolites are mainly CP-5 and catalpol; in first 0.5 h, CP-6 is rapidly hydrolyzed with the relative content decreased ~15%, while after 0.5 h it is generally stable; there are a spot of CP-4, CP-3, CP-2 and CP-1 produced, and this may be due to the esterification of catalpol with the produced metabolite propionic acid¹⁵, or ester

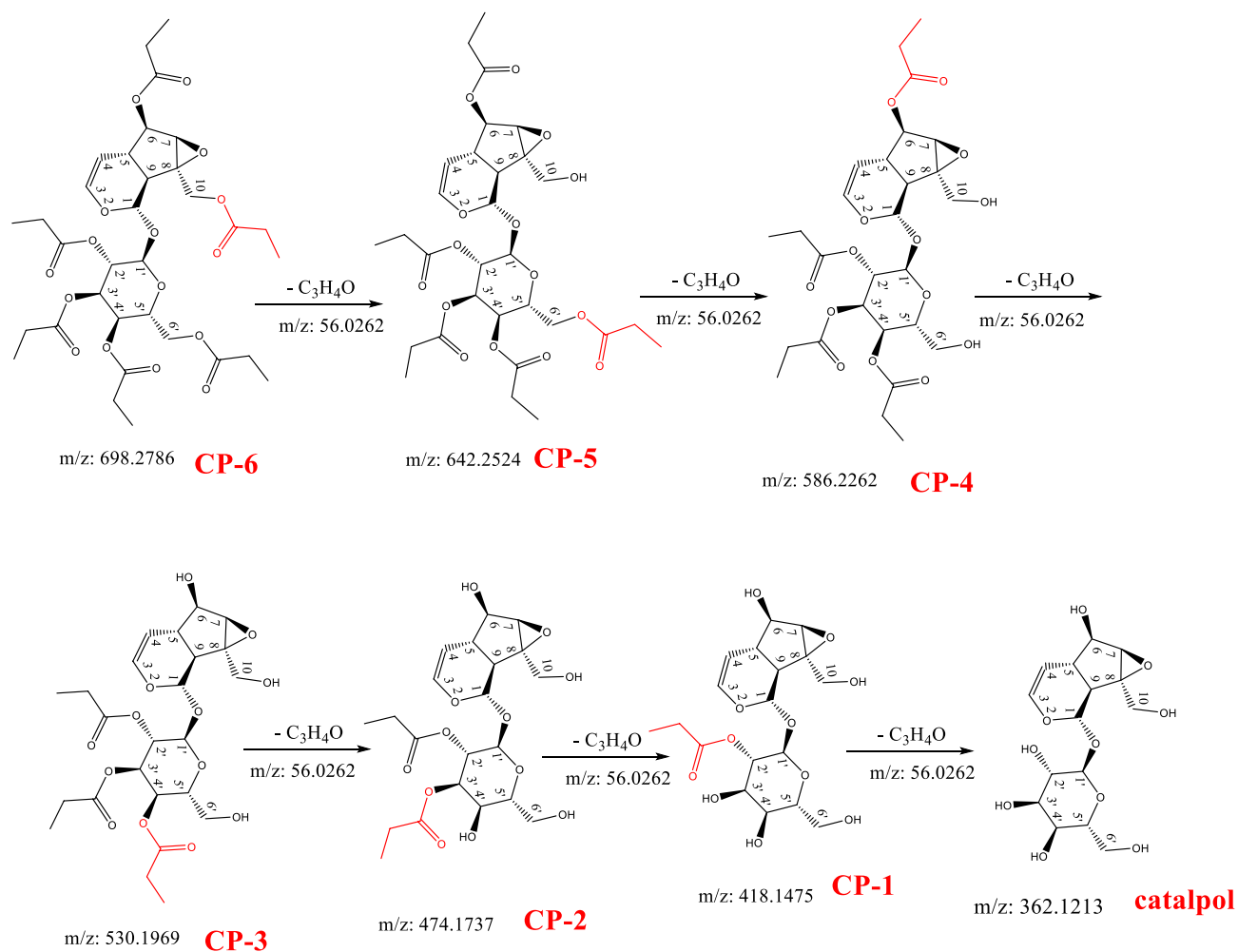


Figure 3. Possible metabolic process of CP-6 under simulated gastric conditions.

No.	Component (M)	Chemical Formula	m/z [M+H] ⁺	m/z [M+NH ₄] ⁺	m/z [M+Na] ⁺
1	CP-6	C ₃₃ H ₄₆ O ₁₆	699.2864	716.3124	721.2678
2	CP-5	C ₃₀ H ₄₂ O ₁₅	643.2602	660.2862	665.2416
3	CP-4	C ₂₇ H ₃₈ O ₁₄	587.234	604.26	609.2154
4	CP-3	C ₂₄ H ₃₄ O ₁₃	531.2047	548.2307	553.1861
5	CP-2	C ₂₁ H ₃₀ O ₁₂	475.1815	492.2075	497.1629
6	CP-1	C ₁₈ H ₂₆ O ₁₁	419.1553	436.1813	441.1367
7	Catalpol	C ₁₅ H ₂₂ O ₁₀	363.1291	380.1551	385.1105

Table 1. Chemical formula and theoretical mass of ionized debris.

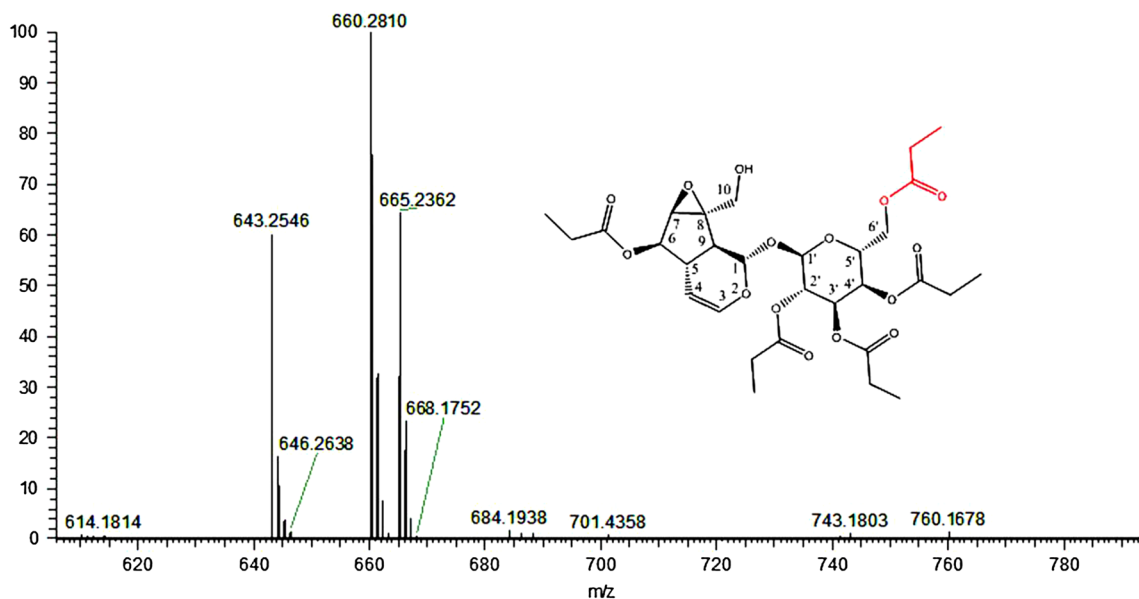


Figure 4. Experimental obtained HRMS in a mixed peak.

No.	Metabolite (M)	Chemical Formula	m/z [M+H] ⁺	m/z [M+NH ₄] ⁺	m/z [M+Na] ⁺
1	CP-6	C ₃₃ H ₄₆ O ₁₆	699.2803	716.3065	721.2617
2	CP-5	C ₃₀ H ₄₂ O ₁₅	643.2546	660.2810	665.2362
3	CP-4	C ₂₇ H ₃₈ O ₁₄	587.2290	604.2556	609.2101
4	CP-3	C ₂₄ H ₃₄ O ₁₃	531.2046	548.2304	553.1846
5	CP-2	C ₂₁ H ₃₀ O ₁₂	475.1841	NA*	497.1583
6	CP-1	C ₁₈ H ₂₆ O ₁₁	419.1536	NA	441.1338
7	Catalpol	C ₁₅ H ₂₂ O ₁₀	NA	NA	385.0892

Table 2. Experimental m/z of metabolites at PI mode.

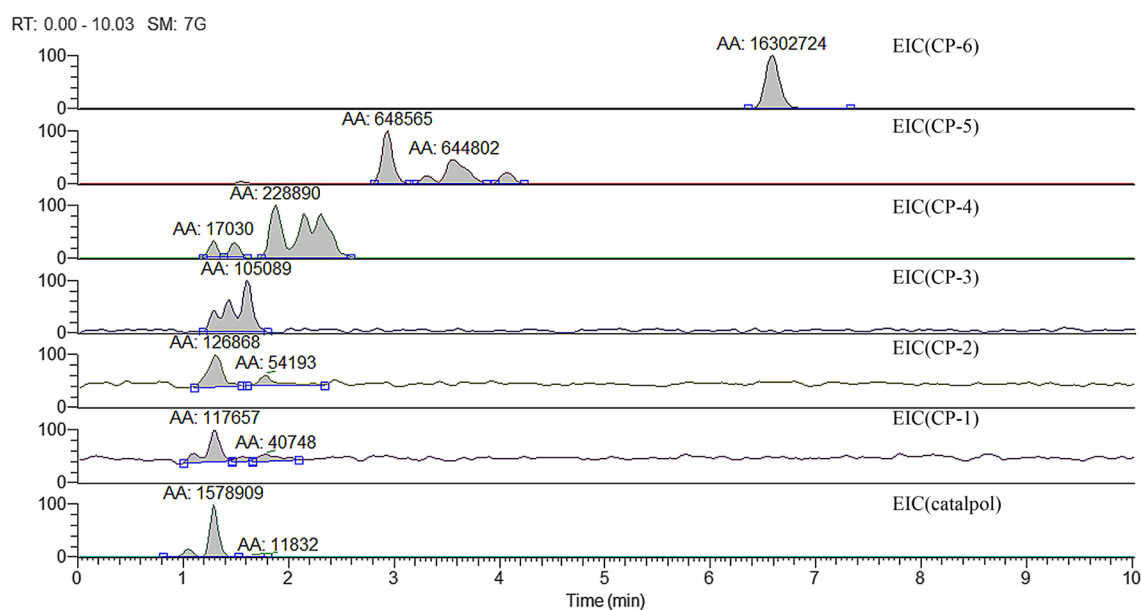


Figure 5. EIC of the metabolites at 3 h.

Time/h	Relative content/%						
	CP-6	CP-5	CP-4	CP-3	CP-2	CP-1	Catalpol
0	99	0	0	0	0	0	0
0.05	91	4	0	0	0	0	5
0.5	84	7	1	0	1	0	6
1.0	83	6	2	0	0	1	8
1.5	88	5	1	0	0	0	5
2.0	83	6	1	0	1	0	9
2.5	82	6	1	0	0	0	10
3.0	81	7	1	1	1	1	8
3.5	82	6	1	0	0	0	10
4.0	84	6	1	1	1	1	7

Table 3. Relative content changes of metabolites within 4 h.

decomposition of C5, C4, C3 and C2. CP-6 and the metabolites are all have potential pharmacological effects which indicate that CP-6 is a prospective drug.

Conclusions

The metabolites of CP-6 under simulated gastric conditions by UPLC-ESI-HRMS were mainly CP-5, catalpol and a spot of CP-4, CP-3, CP-2 and CP-1. The metabolic process of CP-6 may be an hydrolysis under acid conditions. It is rapidly decreased ~ 15% in the first 0.5 h and is generally stable after 0.5 h. The metabolites CP-5, CP-4, CP-3, CP-2, CP-1 and catalpol are all with pharmacological effects¹⁵. Therefore, although CP-6 is metabolized, it still has pharmacological activity. The research results indicate that CP-6 is a prospective drug. This study provides a theoretical basis for the development and utilization of CP-6 as a pharmaceutical preparation.

Data availability

The related data and materials are available from the corresponding author on reasonable request.

Received: 5 February 2020; Accepted: 15 June 2020

Published online: 07 July 2020

References

- Ji, X. Q. *et al.* Changes of catalpol and total iridoid glycosides in roots and leaves of *Rehmannia glutinosa* L. China. *J. Chin. Mater. Med.* **39**, 466–470 (2014).
- Zhao, L. N. *et al.* Catalpol inhibits cell proliferation, invasion and migration through regulating miR-22-3p/MTA3 signalling in hepatocellular carcinoma. *Exp. Mol. Pathol.* **109**, 51–60 (2019).
- Yuan, H. X. *et al.* Effect of catalpol on behavior and neurodevelopment in an ADHD rat model. *Biomed. Pharmacother.* **118**, 109033 (2019).
- Tan, L. L. *et al.* Effects of catalpol on the construction of neurovascular units after cerebral ischemia. *Chin. Pharm. Bull.* **30**, 44–48 (2014).
- Hu, H. M. *et al.* Catalpol inhibits homocysteine-induced oxidation and inflammation via inhibiting Nox4/NF-kappaB and GRP78/PERK pathways in human aorta endothelial cells. *Inflammation* **42**, 64–80 (2019).
- Dong, W. *et al.* Catalpol stimulates VEGF production via the JAK2/STAT3 pathway to improve angiogenesis in rats' stroke model. *J. Ethnopharm.* **191**, 169–179 (2016).
- Wan, D. *et al.* Catalpol stimulates VEGF production via the JAK2/STAT3 pathway to improve angiogenesis in rats' stroke model. *J. Ethnopharm.* **191**, 169–179 (2016).
- Liu, L. *et al.* Catalpol promotes cellular apoptosis in human HCT116 colorectal cancer cells via microRNA-200 and the down regulation of PI3K–Akt signaling pathway. *Oncol. Lett.* **14**, 1168–1177 (2017).
- Lin, C. *et al.* Catalpol protects glucose-deprived rat embryonic cardiac cells by inducing mitophagy and modulating estrogen receptor. *Biomed. Pharmacother.* **89**, 973–982 (2017).
- Zhou, J. *et al.* Catalpol ameliorates high-fat diet-induced insulin resistance and adipose tissue inflammation by suppressing the JNK and NF-κB pathways. *Biochem. Biophys. Res. Commun.* **467**, 853–858 (2015).
- Wang, J. H. *et al.* Catalpol regulates cholinergic nerve system function through effect on choline acetyl-transferase not M receptor affinity. *Biomed. Pharmacother.* **69**, 291–296 (2015).
- Zhang, H. *et al.* Catalpol ameliorates LPS-induced endometritis by inhibiting inflammation and TLR4/NF-kappaB signaling. *J. Zhejiang Univ. Sci. B* **20**, 816–827 (2019).
- Chen, Y. P. *et al.* Loganin and catalpol exert cooperative ameliorating effects on podocyte apoptosis upon diabetic nephropathy by targeting AGES-RAGE signaling. *Life Sci* **252**, 117653 (2020).
- Pungitore, C. R. *et al.* Novel antiproliferative analogs of the Taq DNA polymerase inhibitor catalpol. *Bioorg. Med. Chem. Lett.* **17**, 1332–1335 (2007).
- Dong, C. H. *et al.* Design, synthesis, and preliminary biological evaluation of catalpol propionates as antiangiogenic drugs. *BMC Chem.* **13**(109), 1–11 (2019).
- Dong, C. H., Wang, Q., Wang, G. Q., Chu, M. L. & Zhu, W. M. Propionylation catalpol derivative and preparation method and application thereof: China. CN107739398A [P]. 2018-02-27
- Jiang, S. *et al.* Rapid screening and identification of metabolites of quercitrin produced by the human intestinal bacteria using ultra performance liquid chromatography/quadrupole-time-of-flight mass spectrometry. *Arch. Pharma Res.* **37**, 204–213 (2014).

18. Ma, Z. W. *et al.* Pharmaceutical strategies of improving oral systemic bioavailability of curcumin for clinical application. *J. Control. Rel.* **316**, 359–380 (2019).
19. Meyer, M. R. *et al.* Current status of hyphenated mass spectrometry in studies of the metabolism of drugs of abuse, including doping agents. *Anal. Bioanal. Chem.* **402**, 195–208 (2012).
20. Wang, X. H. *et al.* Human gastrointestinal metabolism of the anti-rheumatic fraction of Dianbaizhu (*Gaultheria leucocarpa* var. *yunnanensis*) in vitro: Elucidation of the metabolic analysis in gastric juice, intestinal juice and human intestinal bacteria by UPLC-LTQ-Orbitrap-MS(n) and HPLC-DAD. *J. Pharm. Biomed. Anal.* **175**, 112791 (2019).
21. Borahan, T. *et al.* A rapid and sensitive reversed phase-HPLC method for simultaneous determination of ibuprofen and paracetamol in drug samples and their behaviors in simulated gastric conditions. *J. Sep. Sci.* **42**, 678–683 (2018).
22. Unutkan, T. *et al.* Development of an analytical method for the determination of amoxicillin in commercial drugs and wastewater samples, and assessing its stability in simulated gastric digestion. *J. Sep. Sci.* **56**, 36–40 (2018).
23. Tao, J. H. *et al.* UPLC-Q-TOF/MS-based metabolic profiles of bioactive components in *Rehmannia glutinosa* and *Cornus officinalis* herb pair by rat intestinal bacteria. *Chin. Herb. Med.* **9**, 147–152 (2017).
24. Yao, J. *et al.* In-vivo and in-vitro metabolism study of timosaponin B-II using HPLC-ESI-MSⁿ. *Chromatographia* **78**, 1175–1184 (2015).
25. Bruins, A. P. Mechanistic aspects of electrospray ionization. *J. Chromatogr. A* **794**, 345–357 (1998).
26. Öztürk Er, E. *et al.* Accurate and sensitive determination of sildenafil, tadalafil, vardenafil, and avanafil in illicit erectile dysfunction medications and human urine by LC with quadrupole-TOF-MS/MS and their behaviors in simulated gastric conditions. *J. Sep. Sci.* **42**, 475–483 (2019).

Acknowledgements

This work was supported by National Natural Science Foundation of China (No. 81373462) and China-Thai Cooperation Project of the National Natural Science Foundation for International Cooperation and Exchange (No. 8151101082).

Author contributions

C.D., G.W., and S.J. moderated and supervised the project. X.C., Q.Z., Z.Z., and Y.S. performed the determination of behavior of CP-6 under the simulated gastric conditions. All authors have read and approved the final manuscript.

Competing interests

The authors declare no competing interests.

Additional information

Correspondence and requests for materials should be addressed to C.D. or G.W.

Reprints and permissions information is available at www.nature.com/reprints.

Publisher's note Springer Nature remains neutral with regard to jurisdictional claims in published maps and institutional affiliations.



Open Access This article is licensed under a Creative Commons Attribution 4.0 International License, which permits use, sharing, adaptation, distribution and reproduction in any medium or format, as long as you give appropriate credit to the original author(s) and the source, provide a link to the Creative Commons license, and indicate if changes were made. The images or other third party material in this article are included in the article's Creative Commons license, unless indicated otherwise in a credit line to the material. If material is not included in the article's Creative Commons license and your intended use is not permitted by statutory regulation or exceeds the permitted use, you will need to obtain permission directly from the copyright holder. To view a copy of this license, visit <http://creativecommons.org/licenses/by/4.0/>.

© The Author(s) 2020